

Physical attributes, limitations, and future potential for PET and SPECT

Ernest V. Garcia, PhD

Advances in SPECT and PET imaging hardware, software, and radiotracers are vastly improving the non-invasive evaluation of myocardial perfusion and function. In contrast to traditional dual-headed, sodium iodide crystal and photomultiplier cameras with mechanical collimators, new SPECT camera designs utilize novel, collimators, and solid-state detectors that convert photons directly to electrical signals. These cameras simultaneously collect data from as many as 76 small detectors narrowly focused on the heart. New noise regularization and resolution recovery/noise reduction reconstruction software interprets emitted counts more efficiently and thus more effectively discriminates between useful signals and noise. As a result, shorter acquisition times and/or lower tracer doses produce higher quality SPECT images than were possible before. PET perfusion imaging has benefitted from the introduction of novel detectors that now allow true 3D imaging, new radiopharmaceuticals, and precise attenuation correction (AC). These developments have resulted in perfusion images with higher spatial and contrast resolution that may be acquired in shorter protocols and/or with less patient radiation exposure than traditional SPECT. Hybrid SPECT/CT and PET/CT cameras utilize transmission computed tomographic (CT) scans for AC, and offer the additional clinical advantages of evaluating coronary calcium, myocardial anatomy (including non-invasive CT angiography), myocardial function, and myocardial perfusion in a single imaging procedure.

Key Words: Solid state cameras • Ultrafast cardiac cameras • Cadmium zinc telluride (CZT) • Resolution recovery • Noise regularization • Hybrid PET/CT • Hybrid PET/MR

INTRODUCTION

Stress-induced myocardial perfusion defects, differentiation of viable from non-viable myocardium, cardiac innervation, and cardiac anatomy are routinely and accurately visualized with single-photon emission computed tomography (SPECT) and positron emission tomography (PET) imaging. New developments in the accuracy, safety, and convenience of the modalities invariably arise from improved methods of detecting the intensity, location, and timing of counts emanating from injected radiopharmaceuticals. This article discusses the tremendous progress in instrumentation that is taking place in myocardial perfusion SPECT and PET imaging and how these innovations are impacting the field.

SPECT IMAGING INSTRUMENTATION

Myocardial perfusion SPECT imaging has enjoyed widespread clinical use because of its well-documented diagnostic accuracy for detecting coronary artery disease. The basic design of the Anger camera, in which a crystal detects gamma rays emitted from a source (the radiopharmaceutical), is more than 50 years old.¹ Vast improvements in hardware, software, and radiotracers have brought cardiac imaging from the simplest planar images to complex, gated, three-dimensional (3D) tomograms capable of reliably estimating the extent, severity, and location of coronary artery disease.

The precision of Anger cameras is limited by their use of mechanical, parallel-hole collimators, and their relatively inefficient use of the sodium iodide (NaI) crystals. In currently available SPECT cameras, gamma rays pass readily through properly aligned holes in a lead collimator to reach the crystal, while radiation coming from a source at an angle is blocked by the lead septa of the holes (Figure 1).² The resolution and count sensitivity of parallel-hole collimators depend on the shape, length, and size of the holes. Longer and narrower holes restrict more photons from reaching the

From the Department of Radiology and Imaging Sciences, Emory University, Atlanta, GA.

Reprint requests: Ernest V. Garcia, PhD, Department of Radiology and Imaging Sciences, Emory University, Atlanta, GA; ernest.garcia@emory.edu.

J Nucl Cardiol 2012;19:S19–29.
1071-3581/\$34.00

Copyright © 2011 American Society of Nuclear Cardiology.
doi:10.1007/s12350-011-9488-3

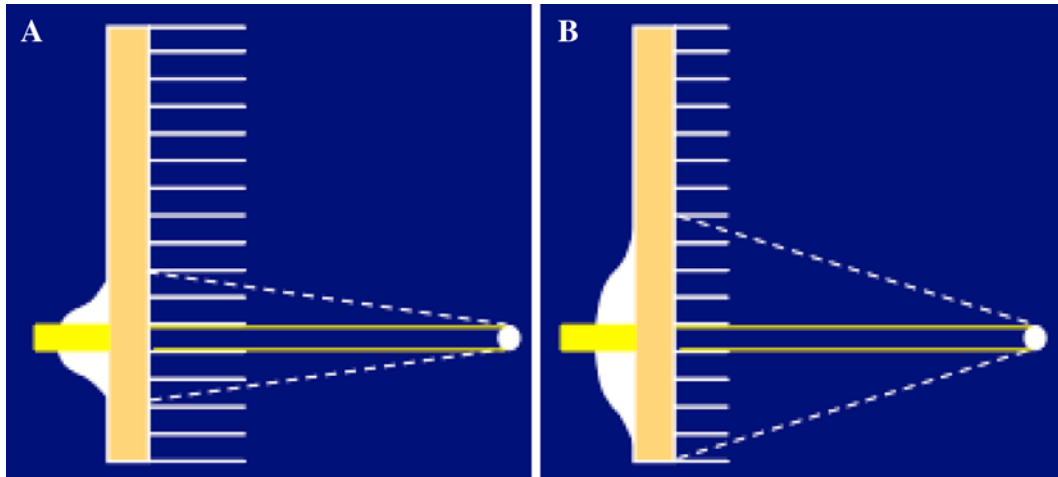


Figure 1. Mechanical collimation. The resolution and count sensitivity of parallel-hole collimators depends on the shape, length, and size of the holes. Each hole in the collimator restricts the photons that may strike the crystal to those that originate within the arc ϕ . **A**, Lengthening the holes of the collimator reduces ϕ and the area exposed through each hole at a given distance. The longer the holes the greater the resolution and the lower the count sensitivity. **B**, Shorter collimator holes decrease resolution. Regardless of the length of the hole the resolution degrades with the distance from the collimator. Reprinted from Garcia and Faber,² edition 2, Copyright 2009, with permission from Elsevier.

crystal, and thus result in greater image resolution, but lower sensitivity. The direction from which the radiation originates can be calculated. Regardless of the length of the hole, image resolution also depends on distance of the source from the collimator. When the source is close to the collimator, radiation passes through fewer collimator holes, thus improving spatial resolution. Moreover, there is less scatter of radiation in the patient than when the source is farther away.

ADVANCES IN SPECT IMAGE RECONSTRUCTION

Recent software improvements in iterative image reconstruction take into account the loss of resolution with distance that is inherent in parallel-hole collimators, and now recover and correctly localize counts that were previously treated as noise. This greater efficiency allows shorter imaging protocols or lower tracer doses to produce higher quality images. Moreover, noise regularization techniques have been implemented which go beyond simple smoothing by considering the expected noise for the regional count density from the specific reconstruction algorithm and filter.^{3,4} When implemented together, these mathematical resolution recovery reconstruction algorithms and noise regularization techniques improve spatial resolution and hence image quality as compared to filtered back projection.

Since resolution recovery requires specific information as to the imaging properties of the system, the recovery algorithm must accurately account for the physical characteristics of the detector, the collimator, and the patient. These recovery algorithms use a database of known detector and collimator characteristics. Recovery also requires specific description of the orbit shape, radius, and/or distance from the patient to the detector.

Most SPECT camera manufacturers have implemented proprietary resolution recovery/noise reduction (RRNR) algorithms into their maximum likelihood expectation maximization or ordered subset expectation maximization iterative reconstruction software. Each of these RRNR algorithms has been validated to various degrees in myocardial perfusion studies trials that compared conventionally reconstructed SPECT images to those reconstructed with RRNR. These studies showed that RRNR-reconstructed images may be acquired in half the time, or with half the injected tracer dose without compromising qualitative or quantitative diagnostic performance,³⁻⁵ whether or not attenuation correction (AC) was applied.⁵ One study showed that high-quality images could be acquired in one quarter of the time if the reconstruction was optimized for the reduced count density.⁶ Left ventricular volumes and ejection fractions of RRNR-reconstructed images were lower, and in one implementation end-systolic volumes were higher as compared to

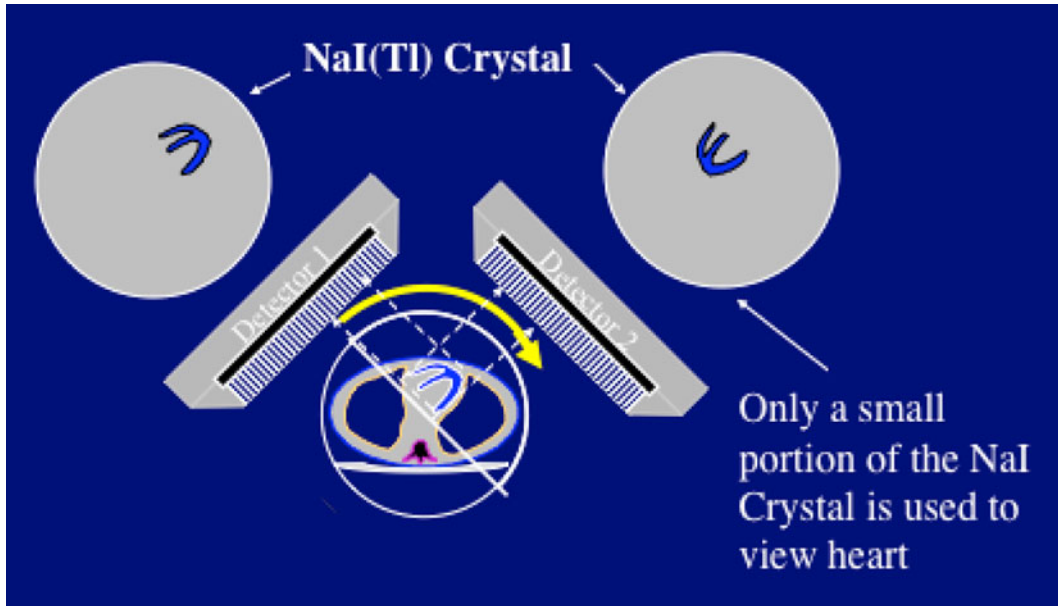


Figure 2. Schematic of conventional 2-detector SPECT cameras. The basic camera design is more than 50 years old. As currently used, two detectors with standard parallel-hole collimators mounted at 90° rotate around the patient. Crystals detect signals from a wide field of view, but only a small portion of the available sodium iodide crystal is utilized to image the heart. Reprinted from Garcia and Faber,² edition 2, Copyright 2009, with permission from Elsevier.

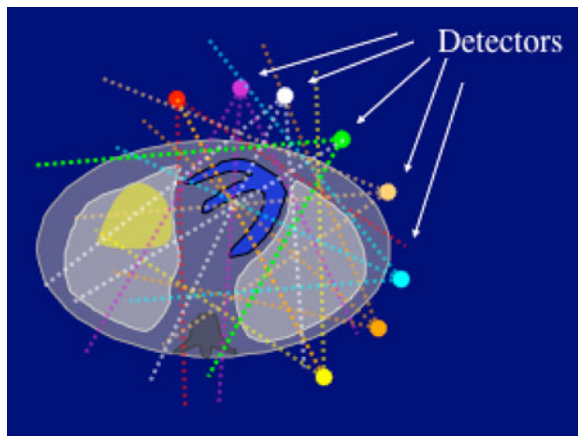


Figure 3. Schematic of detector array in ultra-fast SPECT cameras. Ultra-fast SPECT cameras utilize multiple small detectors that acquire data simultaneously and are constrained to image only the cardiac field of view. This diagram shows eight detectors (represented in different colors) surrounding the patient. These new designs vary in the number and type of scanning or stationary detectors, and whether conventional NaI or newer CZT solid-state detectors are used. They all have in common the potential for a 5- to 10-fold increase in count sensitivity at no loss or even a gain in resolution resulting in the potential for acquiring a stress myocardial perfusion scan injected with a standard dose in 2 minutes or less. Reprinted from Garcia and Faber,² edition 2, Copyright 2009, with permission from Elsevier.

conventionally reconstructed images, but functional results from both techniques were highly correlated.⁴ Importantly, variations of these RRNR algorithms have been implemented in the new ultra-fast camera designs to further improve image spatial and contrast resolution while reducing count noise.

ULTRA-FAST SPECT CAMERA DESIGNS

The original SPECT cameras were developed for use in general nuclear medicine, and did not specifically address the special challenges of imaging the heart. Replacement of the original single-detector systems with two-detector systems enabled faster acquisitions, 3D tomographic reconstruction, ECG gating, and measurement of myocardial function. In two-detector systems, NaI crystals mounted at right angles to each other rotate around the patient at programmable steps, until counts have been acquired from an arc of at least 180° around the heart. Only a small portion of the available NaI crystal area is used to view the heart (Figure 2).² The overall photomultiplier design and the relative inefficiency of the NaI crystals results in limited count sensitivity, limited energy resolution, and limited spatial, and contrast resolution. While SPECT imaging is widely and reliably used, its resolution lags behind that

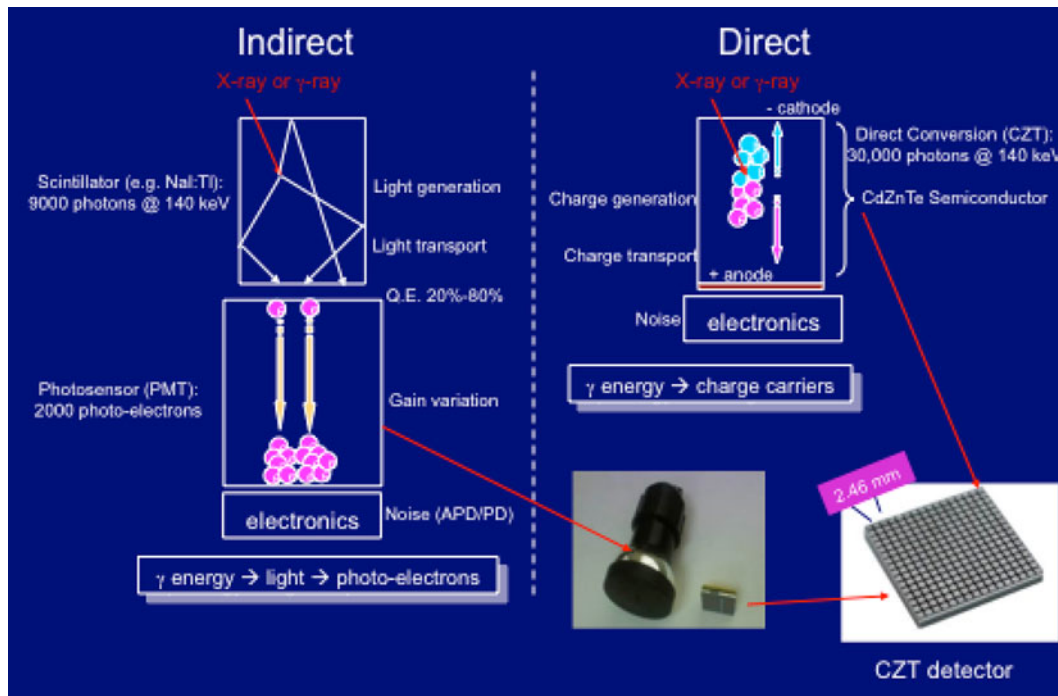


Figure 4. Indirect versus direct conversion of photons to electrical signals. The use of CZT detectors improves the energy and spatial (contrast) resolution, which is especially useful in simultaneous dual isotope imaging protocols. Simultaneously acquired views improve the overall count sensitivity and give complete and consistent angular data needed for both dynamic studies and for the reduction of motion artifacts (image courtesy of Aharon Peretz, PhD).

of magnetic resonance (MR) or computed tomographic (CT) imaging.

A new generation of ultra-fast acquisition cardiac SPECT cameras utilizes as many as 19 smaller detectors that are aligned to specifically target the heart. Smaller detectors and pinhole collimators detect radiation from smaller arcs, which results in improved resolution and higher count sensitivity compared to traditional SPECT (Figure 3).² Since the counts are more efficiently recorded by these cameras, high-quality images can be obtained with fewer counts. If the tracer dose is unchanged, acquisition time can be reduced by half to one-tenth the time required for the traditional camera; if the acquisition time remains unchanged, the tracer dose can be reduced. Motion artifacts are reduced because patients can more easily remain still during shorter acquisition times and because the detectors do not rotate or move axially.

Counts emitted from radiopharmaceuticals have traditionally been recorded “indirectly,” but are now being recorded “directly.” In the conventional systems, gamma rays are converted into visible photons in the NaI crystal, and the visible photons are then converted into electrical pulses by photomultipliers. In the direct conversion systems, cadmium zinc telluride (CZT) semiconductors receive the gamma radiation and

convert the signals directly into electrical signals (Figure 4) within 2.46-mm units. This simpler detection process results in faster and more complete capture of the radiation information within a segment of the heart and thus improves the energy, spatial, and contrast resolution. The improved sensitivity can be especially useful for simultaneous dual-isotope imaging protocols. Ultra-fast scanners that utilize solid-state semiconductors are now commercially available.

The first ultra-fast SPECT system to offer one of these totally different designs was D-SPECT, manufactured by Spectrum Dynamics (Caesarea, Israel).⁷⁻¹⁰ This system uses solid-state CZT detectors mounted on nine vertical columns and placed at 90° to the long axis using 90° geometry. Each of the nine detector assemblies is equipped with a tungsten parallel-hole collimator composed of relatively large (2.46 mm × 2.46 mm), square (vs traditionally cylindrical) collimator holes. The novel shape and size of the holes contribute to the increased count sensitivity of the camera. Each detector assembly is made to fan in synchrony with the other eight detector assemblies while all nine simultaneously image the heart. The patient is imaged in a reclined sitting position, similar to a dentist’s chair, with the patient’s left arm placed on top of the detector housing.

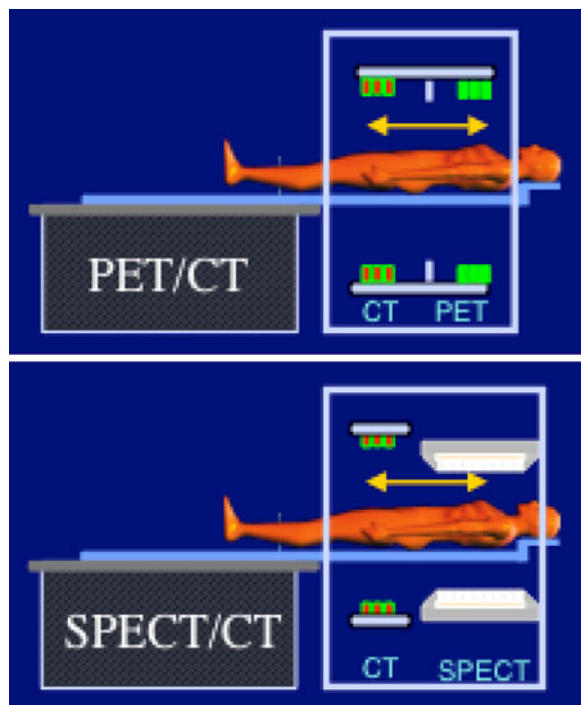


Figure 5. Schematic of hybrid PET/CT and SPECT/CT imaging systems. Hybrid systems now in routine clinical use physically couple a CT scanner with a PET (*top panel*) or a SPECT (*bottom panel*) scanner. The coupled CT scanner can range from 1 to 64 slices and may be used for AC, to evaluate coronary calcium and/or to perform CT angiographic studies. These systems can provide, in one imaging study, comprehensive cardiac evaluation of anatomic information from the CT scan and physiologic information from the PET or SPECT scans. Reprinted from Garcia and Faber,²⁰ Figure 5, Copyright 2009 with kind permission of Springer Science and Business Media.

The second SPECT system to offer a revolutionary new design is the system developed by GE Healthcare (Waukesha, WI)¹¹⁻¹⁸ known as the Discovery Nuclear Medicine 530c system. This SPECT system design uses Alcyone™ technology that consists of an array of 19 pinhole collimators, each with four solid-state CZT pixilated detectors that simultaneously image the heart; there are no moving parts during data acquisition. Nine of the pinhole detectors are oriented perpendicular to the patient's long axis while five are angulated above and five below the axis for true 3D acquisition geometry. The use of simultaneously acquired views improves the overall sensitivity and provides complete and consistent angular data needed for acquisition of dynamic functional data and for the reduction of motion artifacts. In addition, attenuation artifacts may be reduced because not all views are acquired through the attenuator (e.g., breast); some views of the heart are acquired from above or below the breast attenuator. The detector assembly is

mounted on a gantry, which allows for patient positioning in the supine or prone positions. A hybrid system (570c) is also available with a volumetric CT scanner to facilitate AC and to incorporate CT applications. Iterative reconstruction adapted to this geometry is used to create transverse axial slices of the heart and to perform AC.

HYBRID PET/CT AND SPECT/CT IMAGING SYSTEMS

Hybrid systems that physically couple a CT scanner with either a PET or a SPECT scanner are now in routine clinical use (Figure 5).^{19,20} Coupled CT scanners are commonly used for AC, and may also be used to evaluate coronary calcium and/or perform CT angiographic studies. An advantage of these systems is that they can provide, in one imaging study, comprehensive cardiac evaluation of anatomic information from the CT scan and physiologic information from the PET or SPECT scan.²¹ This benefit comes at a cost of additional quality control related to the differences between how AC is performed using a CT transmission scan versus a rotating radioactive line scan. Since these issues are common to both PET and SPECT, they will be covered once in the PET section.

PET IMAGING PRINCIPLES

A positron is an antimatter particle—a positively charged electron. When emitted, a positron travels through matter and loses its kinetic energy. Under ideal conditions, the positron and its antiparticle, an electron, drift towards each other. When they contact each other, the mass of two electrons is converted to energy via Einstein's famous equation $E = mc^2$ through the pair annihilation process. The resting mass of the positron plus its opposing electron multiplied by the speed of light (c) squared are each converted to 511-keV gamma energy. Because there is zero momentum when they touch, the two photons are discharged along the same collinear ray in exactly opposite directions (Figure 6).¹⁹ Gamma rays resulting from the annihilation are localized with the principles of coincidence detection by the PET scanner. Therefore, radiation-absorbing mechanical collimators are not necessary. PET systems are more efficient and can detect more counts per unit of injected dose than SPECT systems.

Positrons with higher kinetic energy travel longer than positrons with low kinetic energy before interacting with an electron in an annihilation event, in which their combined masses are converted to energy. When the positron and electron pairs touch, they still produce a of

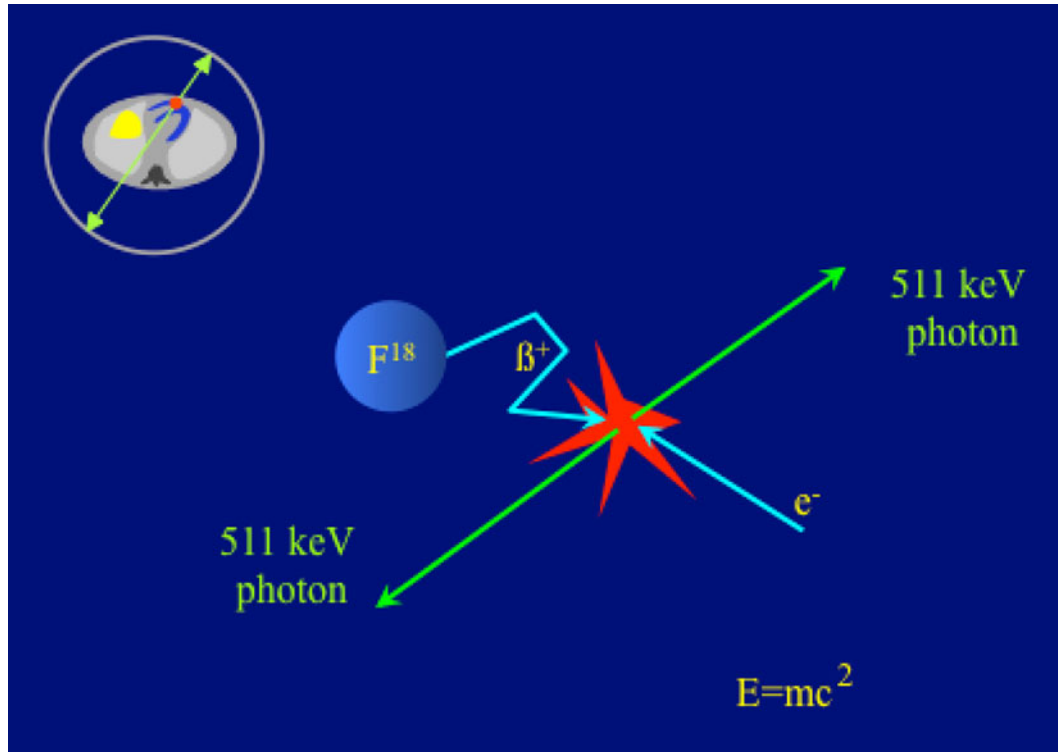


Figure 6. Principle of positron annihilation. PET cameras detect paired gamma rays (511 keV of energy each) produced by positron annihilations. The paired gamma rays are discharged in exactly opposite directions along the same ray. Positron decay can be localized with the use of the principles of coincidence detection. Without mechanical collimation, PET cameras detect counts more efficiently than SPECT systems. *Inset* shows how the two 511-keV photons are used to localize the radioactive event using electronic collimation. Garcia et al,¹⁹ Figures 1-3, Copyright 2009 with kind permission of Springer Science and Business Media.

2×511 keV energy, but because of residual kinetic energy the two 511-keV photons may not necessarily be discharged in exactly opposite directions. An energetic positron will transfer more than 511 keV, and so the resulting photons will not be discharged along the same ray. Depending on the residual momentum, the photons may be emitted as much as a half-degree away from 180° of each other (Figure 7). Resolution of PET images is ultimately determined by the distance the positron travels from the emitted nucleus to the point of annihilation (positron range), the residual kinetic energy at the time of pair annihilation, random counts, and the finite thickness of the detectors.^{19,22} The physics of fluorine (^{18}F) and rubidium (^{82}Rb) predict that ^{18}F would provide higher resolution than ^{82}Rb because fluorine's positron range (0.6 mm) is considerably lower than that of rubidium (4 mm). Theoretically, imaging in a strong magnetic field can reduce the positron range and kinetic energy of the emitted photon, thus increasing resolution; this may represent a potential benefit of hybrid PET/MR systems.

ADVANCES IN PET INSTRUMENTATION

Improvements in gantry and detector design and the availability of true 3D imaging represent the most important advances in PET instrumentation. Compared to conventional bismuth germanate (BGO) scintillation crystals, newer lutetium oxyorthosilicate (LSO), lutetium-yttrium oxyorthosilicate (LYSO), and cerium-doped gadolinium oxyorthosilicate (GSO:Ce) crystals have higher light outputs and significantly shorter decay constants. The higher light output results in improved energy and spatial resolution, while the faster decay reduces random coincidences that affect the counting rate capabilities of the system.

The ability to perform 3D imaging represents a major step forward for PET imaging. Two-dimensional (2D) detectors are equipped with lead septa that act like collimators along cross-transverse axial planes. With these septa in place, there is coincidence only within a single ring of detectors. Removal of the shields (septa) between rings in 3D imaging greatly increases count rate

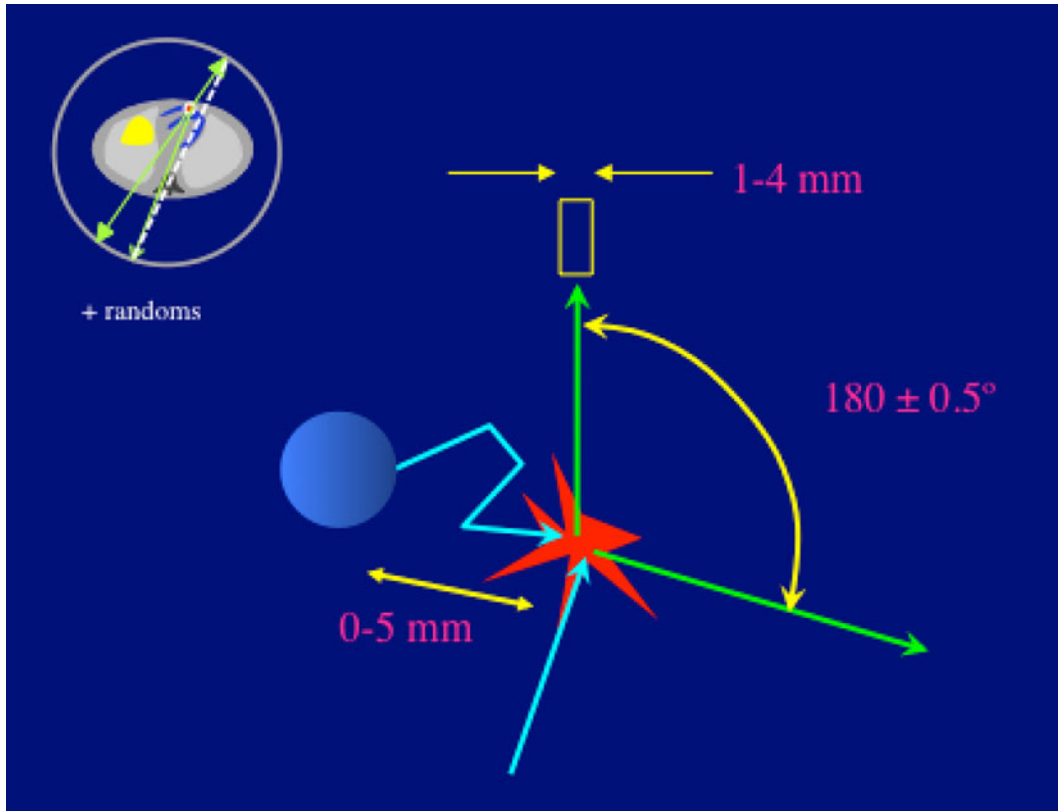


Figure 7. Limitations in PET resolution. This figure illustrates why resolution is lost in actual PET imaging. Resolution losses are due to: the travel of the positron from the emitted nucleus, the residual kinetic energy at the time of pair annihilation, the finite thickness of the detectors, and random radiation. *Inset* shows how the reconstructed ray (*dashed line*) does not cross the location of the emitted positron.

and allows coincidence not only within rings but also between rings as well (Figure 8).¹⁹ This coincidence between rings and the absence of lead collimation result in 3D PET imaging being much more sensitive than SPECT, particularly in the center of the scanner. Compared to 2D PET, the higher count sensitivity of 3D PET allows injection of lower doses of radiopharmaceuticals.

NEED FOR AC IN PET

The gamma energy levels of PET radiotracers (511 keV) are considerably higher than those of ^{99m}Tc-labeled radiopharmaceuticals (140 keV) and thallium-201 (70-90 keV) used in SPECT imaging. The complications of imaging single photons in SPECT are compounded by having to image two photons in PET to locate an annihilation event. When they pass through soft tissue, the two 511-keV photons must be detected in coincidence before the direction of the radiation event (which is necessary to create the images) can be recorded. Thus, even though each 511-keV photon is

attenuated less than a single 140-keV ^{99m}Tc photon, the fact that two photons must be recorded in PET means that there is more attenuation in PET than SPECT. Because the two photons project along the same ray, they must travel through the same total amount of tissue regardless of where along that ray they were emitted. Therefore, the total measured attenuation in PET is exactly the same anywhere along this line. In SPECT imaging, there is no opposing photon to assist in localizing an annihilation event, so attenuation varies exponentially. These phenomena translate to a very simple algorithm for correcting attenuation from PET images and a very complicated one for SPECT. Unlike SPECT, PET data can be accurately corrected for attenuation by simply multiplying each projection line with the appropriate AC factor determined from a transmission germanium-68 line source. Advanced software effectively manages these challenges. The method by which this is accomplished is diagrammed in Figure 9, which shows that a theoretical blank emission scan acquired without the patient in the camera may yield 100 counts. Repeating the emission scan with the

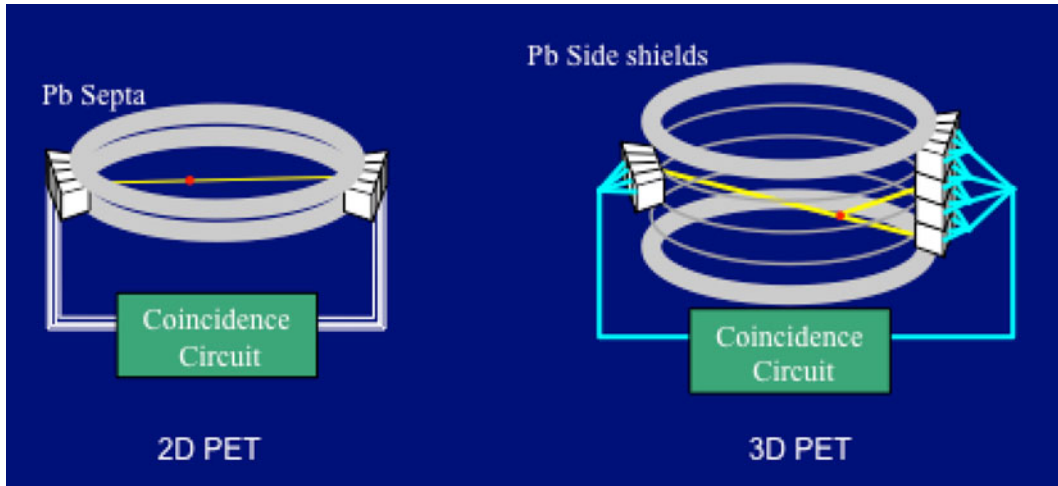


Figure 8. 2D versus 3D PET acquisition. 2D PET systems, equipped with lead septa, only accept coincidences from crystals in the same ring of detectors. 3D PET systems, by removing the septa, accept coincidences in any ring and greatly increase count rate and sensitivity. The difficulties associated with removing the septa are: more scatter; more random events; and increased count rate; these greatly increase dead time. 3D PET cardiac imaging must compensate for these problems. Reprinted from Garcia et al,¹⁹ Figures 1-37, Copyright 2009 with kind permission of Springer Science and Business Media.

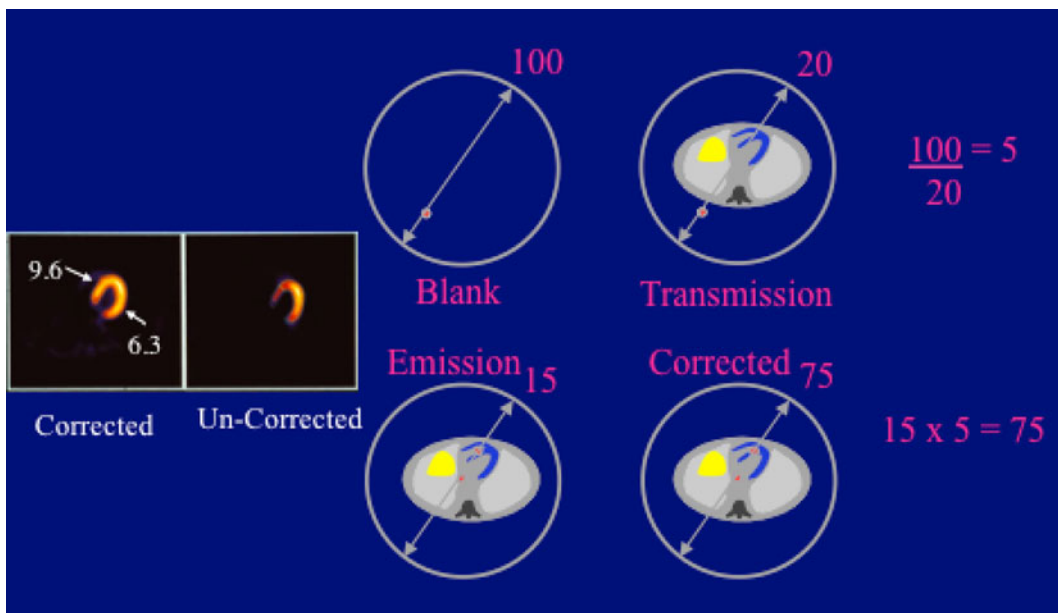


Figure 9. PET AC using Ge-68 radioactive line source. PET AC uses simple matrix algebra by dividing the counts from the blank scan by the counts from the transmission scan multiplied by the counts from the emission scan with the patient. Image *inset* illustrates the dramatic differences in left ventricular count distribution before and after being corrected for AC.

patient in the camera yields 20 counts, resulting in an attenuation factor of five. If the patient's emission scan shows 15 counts along a ray, the attenuation-corrected number will be 15×5 or 75 counts.^{19,22} Accurate AC

for both PET and SPECT requires measurement of patient-specific attenuation maps. PET imaging must always include AC. The dramatic differences in quality between the non-corrected ¹⁸F-fluorodeoxyglucose

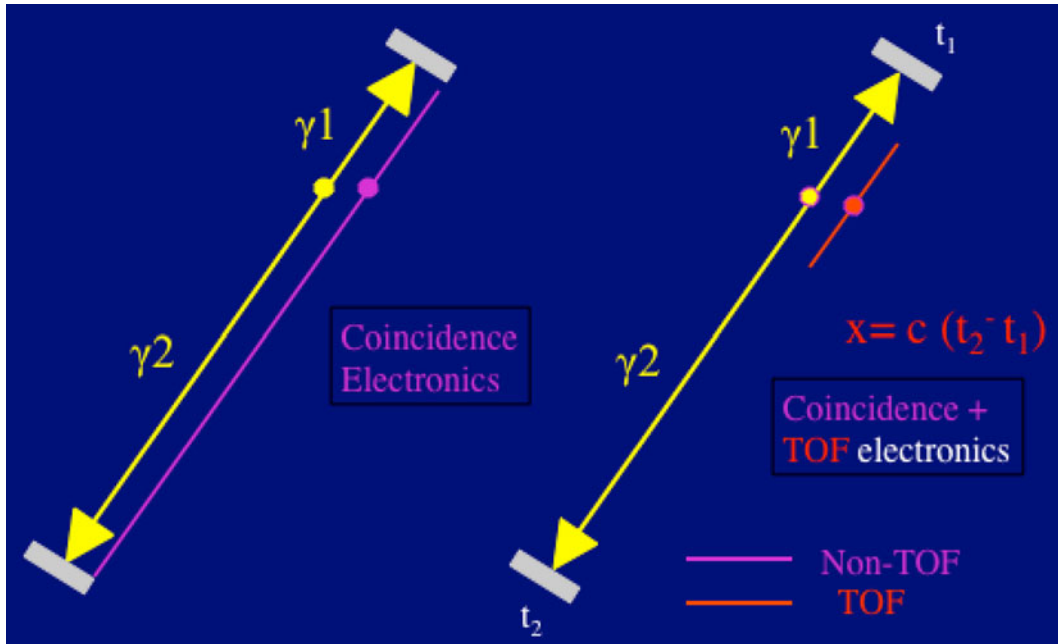


Figure 10. Non-TOF versus TOF Imaging. In TOF imaging the difference in the time when the two detectors record the annihilation event multiplied by the speed of light positions the event along the backprojected line. In TOF, instead of backprojecting an entire line only the line segment corresponding to the time window of the event is projected. This results in increased lesion contrast in TOF versus non-TOF imaging.

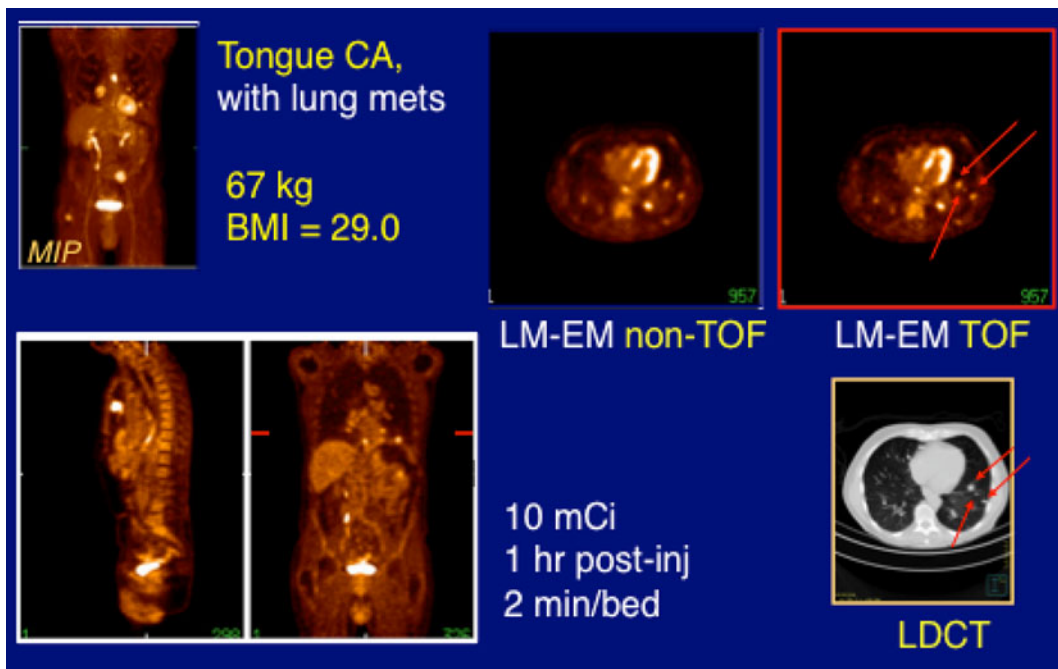


Figure 11. Comparison of lesion contrast in iterative reconstruction non-TOF versus LMEM TOF in a patient with lung metastasis. Note the improvement in lesion contrast indicated by the red arrows. The benefits of this technology have not yet been applied to cardiac imaging because of concurrent heart and lung motion. Visualization by LDCT is shown for comparison (images courtesy of Joel Karp, PhD). *LM-EM*, List mode-expectation maximization; *TOF*, time-of-flight; *CA*, carcinoma; *mets*, metastases; *LDCT*, low-dose spiral computer tomography.

(FDG) transverse axial slice and after applying AC factors of 9.6 to the septal wall and 6.3 to the lateral wall are readily apparent (Figure 9).

AC during PET myocardial perfusion imaging has traditionally been performed by measuring the attenuation of 511-keV photons with a germanium-68 radioactive line source. Unfortunately, the ^{68}Ge line sources decay and are expensive to replace. An advantage of hybrid PET/CT systems is that AC is performed with CT and CT produces the same quality transmission images over time with a fixed initial cost. A disadvantage is that the CT attenuation image is acquired very rapidly, and thus does not account for the changes in attenuation seen over the course of patient breathing cycles. Therefore, mis-registration of the emission versus perfusion scans can result in significant errors in AC. Moreover, since the transmission scan is measured with the continuous energy spectrum of x-rays, there is a small but measureable error in converting the x-ray attenuation to the mono-energetic 511-keV photons that are attenuated in PET. Experimental hybrid PET/MR systems under development offer the promise of simultaneous acquisition of both PET and MR data, which is expected to improve registration, and thus provide better AC than is currently available.

TIME-OF-FLIGHT (TOF)

The coincidence electronics in advanced PET scanners with TOF electronics are capable of measuring the time interval between one photon hitting one detector and the second photon from the same annihilation event hitting an opposing detector. That difference in time multiplied by the speed of light estimates the location of the annihilation event along the coincidence ray between the two detectors (Figure 10).²³ This allows TOF scanners to localize an annihilation event to a much smaller directional ray than conventional PET scanners, and results in increased spatial resolution. To date, this improvement has not been applied to cardiac imaging because of cardiac motion during contraction and chest motion during breathing. Nevertheless, the advent of respiratory gating and freeze-motion algorithms should eventually improve the image quality of cardiac studies acquired on TOF systems compared to conventional non-TOF PET systems (Figure 11).

SUMMARY

The most recent advances in SPECT imaging are seen in the ultra-fast scanners now available. Instead of two large, movable detectors encircling a supine patient, the latest systems include multiple, small, solid-state detectors arranged in a configuration around a reclining

patient's chest. Fewer motion artifacts occur because of the shortened image acquisition times and patient position, and high-quality, high-resolution images are acquired with lower doses of radiation.

Theoretically, compared to SPECT, PET is limited in resolution because of increased attenuation and positron range. But in practice, PET instrumentation is developed to a much higher degree. PET images have higher spatial resolution, more accurate AC, and hence better resolution and quantification than SPECT images. Increased availability of hybrid PET/MR and PET/CT perfusion imaging systems, higher count sensitivity, and incorporation of advanced respiratory gating and TOF capability will further improve PET quality.

Disclosure

Dr Garcia reported receiving grant support from GE Healthcare and the National Institutes of Health. He reported receiving royalties from Emory Cardiac Toolbox, PERFEX, Heartfusion, Synctool, ExSPECT II, and Books. He reported stock ownership in Syntermed, Inc. He reported to be a consultant of Syntermed, Lantheus Medical Imaging, and GE Healthcare.

References

1. Anger HO. Scintillation camera. *Rev Sci Instrum* 1958;29:27-33.
2. Garcia EV, Faber TL. New trends in camera and software technology in nuclear cardiology. *Cardiol Clin* 2009;27:227-36.
3. Borges-Neto S, Pagnanelli RA, Shaw LK, Honeycutt E, Schwartz SC, Adams GL, et al. Clinical results of a novel wide beam reconstruction method for shortening scan time of Tc-99m cardiac SPECT perfusion studies. *J Nucl Cardiol* 2007;14:555-65.
4. DePuey EG, Gadraju R, Clark J, Thompson L, Anstett F, Shwartz SC. Ordered subset expectation maximization and wide beam reconstruction "half-time" gated myocardial perfusion SPECT functional imaging: A comparison to "full-time" filtered back-projection. *J Nucl Cardiol* 2008;15:547-63.
5. Venero CV, Heller GV, Bateman TM, McGhie AI, Ahlberg AW, Katten D, et al. A multicenter evaluation of a new post-processing method with depth-dependent collimator resolution applied to full-time and half-time acquisitions with and without simultaneously acquired attenuation correction. *J Nucl Cardiol* 2009;16:714-25.
6. DePuey EG, Bommireddipalli S, Clark J, Thompson L, Srour Y. Wide beam reconstruction "quarter-time" gated myocardial perfusion SPECT functional imaging: A comparison to "full-time" ordered subset expectation maximization. *J Nucl Cardiol* 2009;16:736-52.
7. Sharir T, Ben-Haim S, Merzon K, Prochorov V, Dickman D, Ben-Haim S, et al. High-speed myocardial perfusion imaging: Initial clinical comparison with conventional dual detector Anger camera imaging. *J Am Coll Cardiol Cardiovasc Imaging* 2008;1:156-63.
8. Sharir T, Slomka PJ, Hayes SW, DiCarli MF, Ziffer JA, Martin WH, et al. Multicenter trial of high-speed versus conventional single-photon emission computed tomography imaging: Quantitative results of myocardial perfusion and left ventricular function. *J Am Coll Cardiol* 2010;55:1965-74.

9. Berman DS, Kang X, Tamarappoo B, Wolak A, Hayes SW, Nakazato R, et al. Stress thallium-201/rest technetium-99m sequential dual isotope high-speed myocardial perfusion imaging. *J Am Coll Cardiol Cardiovasc Imaging* 2009;2:273-82.
10. Ben-Haim S, Kacperski K, Hain S, VanGramberg D, Hutton BF, Erlandsson K, et al. Simultaneous dual-radionuclide myocardial perfusion imaging with a solid-state dedicated cardiac camera. *Eur J Nucl Med Mol Imaging* 2010;37:1710-21.
11. Garcia EV, Tsukerman L, Keidar Z. A new solid-state ultra fast cardiac multi-detector SPECT system. *J Nucl Cardiol* 2008;15:S3. (abstract).
12. Esteves FP, Raggi P, Folks RD, Keidar Z, Askew JW, Rispler S, et al. Novel solid-state-detector dedicated cardiac camera for fast myocardial perfusion imaging: Multicenter comparison with standard dual detector cameras. *J Nucl Cardiol* 2009;16:927-34.
13. Buechel RR, Herzog BA, Husmann L, Burger IA, Pazhenkottil AP, Treyer V, et al. Ultrafast nuclear myocardial perfusion imaging on a new gamma camera with semiconductor detector technique: First clinical validation. *Eur J Nucl Med Mol Imaging* 2010;37:773-8.
14. Herzog BA, Buechel RR, Katz R, Brueckner M, Husmann L, Burger IA, et al. Nuclear myocardial perfusion imaging with a cadmium-zinc-telluride detector technique: Optimized protocol for scan time reduction. *J Nucl Med* 2010;51:46-51.
15. Buechel RR, Pazhenkottil AP, Herzog BA, Husmann L, Nkoulou RN, Burger IA, et al. Real-time breath-hold triggering of myocardial perfusion imaging with a novel cadmium-zinc-telluride detector gamma camera. *Eur J Nucl Med Mol Imaging* 2010; 37:1903-8.
16. Pazhenkottil AP, Buechel RR, Herzog BA, Nkoulou RN, Valenta I, Fehlmann U, et al. Ultrafast assessment of left ventricular dyssynchrony from nuclear myocardial perfusion imaging on a new high-speed gamma camera. *Eur J Nucl Med Mol Imaging* 2010;37:2086-92.
17. Herzog BA, Buechel RR, Husmann L, Pazhenkottil AP, Burger AP, Wolfrum M, et al. Validation of CT attenuation correction for high-speed myocardial perfusion imaging using a novel cadmium-zinc-telluride detector technique. *J Nucl Med* 2010;51:1539-44.
18. Pazhenkottil AP, Husmann L, Kaufmann PA. Cardiac hybrid imaging with high-speed single-photon emission computed tomography/CT camera to detect ischaemia and coronary artery obstruction. *Heart* 2010;96:2050.
19. Garcia EV, Galt R, Faber TL, Chen J. Principles of nuclear cardiology. In: Dilsizian V, Narula J, editors. *Atlas of nuclear cardiology*. 3rd ed. Philadelphia: Current Medicine LLC; 2009. p. 1-36.
20. Garcia EV, Faber TL. Advances in nuclear cardiology instrumentation. Clinical potential of SPECT and PET. *Curr Cardiol Imaging Rep* 2009;2:230-7.
21. Santana CA, Garcia EV, Faber TL, Sirineni GKR, Esteves FP, Sanyal R, et al. Diagnostic performance of fusion of myocardial perfusion and computed tomography coronary angiography. *J Nucl Cardiol* 2009;16:201-11.
22. Cherry SR, Sorenson JA, Phelps ME. *Physics in nuclear medicine*. 3rd ed. Philadelphia: Saunders; 2003. p. 333.
23. Karp JS, Surti S, Daube-Witherspoon ME, Muehlelehner G. Benefit of time-of-flight in PET: Experimental and clinical results. *J Nucl Med* 2008;49:462-70.